

UCLA

UCLA Previously Published Works

Title

Experimental investigation of bidensity slurries on an incline

Permalink

<https://escholarship.org/uc/item/7sq3m4gr>

Journal

Granular Matter, 16(2)

ISSN

1434-5021

Authors

Lee, Sungyon
Mavromoustaki, Alik
Urdaneta, Gilberto
[et al.](#)

Publication Date

2014-04-01

DOI

10.1007/s10035-013-0480-2

Peer reviewed

Experimental investigation of bidensity slurries on an incline

Sungyon Lee · Aliko Mavromoustaki · Gilberto Urdaneta · Kaiwen Huang · Andrea L. Bertozzi

Received: date / Accepted: date

Abstract We investigate the dynamics of bidensity slurries on an incline. The particle-fluid mixture consists of two species of negatively buoyant particles that have roughly the same size but significantly variant densities. This mismatch in particle densities induces or prevents settling depending on the relative amount of heavy to light particles, leading to complex regimes also found in the monodisperse case. In addition, when settling effects dominate within the thin film, we observe the phase separation down the incline between the particles and the liquid, as well as between two particle types.

Keywords particle-laden flow · thin films · bidisperse slurries · shear-induced migration · particle segregation

1 Introduction

In recent years, there has been much focus on the gravity-driven, free-surface flows of a particle-fluid mixture both experimentally and theoretically [1–6], due to their relevance in geophysical phenomena (i.e. landslides [7,8]) and industrial applications. Experiments in [1,3,5] revealed complex dynamics of the monodisperse slurry depending on the total volume fraction, ϕ_0 , and channel inclination angle, α . At low inclination angles and particle concentrations (i.e. $\alpha < 35^\circ$ and $\phi_0 < 0.35$), the particles settle in the direction normal to the channel walls as they move down the incline, resulting in the ‘settled’ regime. For $\alpha > 40^\circ$ and $\phi_0 > 0.4$, more particles collect near the free surface, corresponding to

the ‘ridged’ regime. For the intermediate parameter values, the particles appear to be evenly distributed inside the thin film, yielding the transient ‘well-mixed’ regime. This behavior was explained theoretically based on a diffusive flux model in [2–4], which included the competing effects of gravity and varying shear.

The dynamics of bidisperse suspensions has also been investigated in the low Reynolds number limit but has thus far excluded the thin, free-surface flow geometry. Previous studies include the sedimentation of bidisperse suspensions, which revealed the enhanced settling of heavy particles with the addition of lighter ones [9–12]. Bidisperse slurries have also been studied in the constant shear flow, as Tripathi and Acrivos [13] investigated the resuspension behavior of a bidisperse mixture in a Couette device.

In this paper, we investigate the dynamics of a thin layer of bidensity mixture flowing down an incline due to gravity. Distinct from the previous bidisperse studies, this current geometry incorporates the effects of both gravitational sedimentation and varying shear inside the thin film. In particular, we identify the three aforementioned regimes (settled, well-mixed, and ridged) experimentally as evident in the monodisperse case and focus on the effects of including a second particle species. This work is consequential in light of numerous industrial applications (such as mineral processing via spiral separators) that involve segregating particles of different densities. Recent work on spiral separators showed that, to leading order, the diffusive flux model for monodisperse slurries is valid even in a spiral geometry [14,15]. This allowed Lee *et al.* [14,15] to develop a simple model for particle segregation in the spiral separator for monodisperse suspensions. Thus, the current work on bidensity mixtures provides fundamental groundwork, essential in investigating the multi-species

Aliko Mavromoustaki
UCLA Mathematics Department, Box 951555
Los Angeles, CA 90095-1555, USA
Tel.: +1-310-825-8525
E-mail: aliki@ucla.edu

segregation mechanism in more complex geometries. The paper is organized as follows: Sec. 2 describes the experimental setup and procedure; Sec. 3 discusses the experimental results, followed by the discussion of future work in Sec. 4.

2 Experimental setup

The experimental apparatus (see Fig. 1) consists of an acrylic track of length 90 cm and width 14 cm with an adjustable inclination angle, α . A reservoir of volume $6 \cdot 10^{-4} \text{ m}^3$ sits on top of the incline with a release gate that leads to the track. A slurry mixture of 100 ml in volume is emptied into the reservoir and flows down the track once the release gate is lifted. A digital camera mounted in front of the incline captures the motion of the mixture in a 12-20 minute long video from the time it is first released from the reservoir to when it reaches the bottom of the track. The runs are repeated 2-3 times. Each video is subsampled into a series of images that are one second apart, and the images are subsequently analyzed using MATLAB[®].

The fluid used in all the experiments is PDMS oil (Clearco Products) with density $\rho_l = 970 \text{ kg/m}^3$ and kinematic viscosity $\nu = 10^{-3} \text{ m}^2/\text{s}$, which is approximately 1000 times more viscous than water. Two types of beads are present in the suspension, which sets this investigation apart from the previous monodisperse experiments in the same geometry [3–5]. The glass beads (Ceroglass, P1) have density of $\rho_{p1} = 2500 \text{ kg/m}^3$ and average diameter of $d_1 = 380 \text{ nm}$. The second species of particles is ceramic beads (Ceroglass, P2) with $\rho_{p2} = 3800 \text{ kg/m}^3$ and $d_2 = 300 \text{ nm}$. While both types of particles are negatively buoyant ($\rho_l < \rho_{p1} < \rho_{p2}$), the ceramic beads (P2) are 1.5 times heavier than the glass particles (P1) and hence settle faster. The particle diameters on average differ by 6% and are considered constant (i.e. $d \approx d_1 \approx d_2$) for the purposes of data interpretation. In the experimental pictures presented in this manuscript, the glass and ceramic beads are shown as red and blue, respectively, while, in selected runs, the oil is dyed yellow for better visualization. The specifications of materials used are listed in Table 1.

We carry out a series of experiments in which we vary two system parameters: inclination angle α , and the volume ratio between glass and ceramic beads, denoted by λ . The latter is defined by $100\% \cdot [V_{p1}/(V_{p1} + V_{p2})]$, where V_{p1} and V_{p2} are the volumes of glass and ceramic beads, respectively. The total volume fraction of particles is given by $\phi_0 = V_p/(V_p + V_l)$, where V_l is the liquid volume and $V_p = V_{p1} + V_{p2}$. While preliminary experiments have also been conducted for $\phi_0 = 0.2$

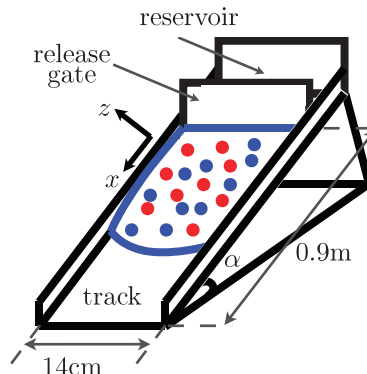


Fig. 1 Schematic of the experimental apparatus.

Table 1 Experimental parameters used

| particles | d (mm) | ρ_p (kg/m ³) |
|--------------------|---------------------------|-------------------------------|
| P1 (glass, red) | 0.25-0.50 | 2500 |
| P2 (ceramic, blue) | 0.20-0.40 | 3800 |
| fluid | ν (m ² /s) | ρ_l (kg/m ³) |
| PDMS oil (yellow) | 10^{-3} | 970 |

and $\phi_0 = 0.5$, the results reported in Sec. 3 focus only on the $\phi_0 = 0.4$ case.

3 Experimental results

In what follows we describe the regimes observed in gravity-driven, particle-laden flow. As mentioned in Sec. 1, we observe three distinct regimes, which arise due to competition between two governing physical effects: settling due to gravity and shear-induced migration. The latter effect causes the particles to move towards low shear-stress regions [16, 17], which results in particle re-suspension towards the free surface. In situations where gravitational effects dominate (i.e. at low values of α and ϕ_0), the particle-laden flow reaches the ‘settled’ regime, in which the particles settle rapidly to channel walls, leaving the clear fluid on top. Since the flow is generally faster near the free surface, the liquid on top travels ahead of the particles, forming clear fingers at the leading edge. Experimentally, the settled regime is characterized by a clear fluid front (see top row of Fig. 2). In situations where shear-induced migration dominates (i.e. at higher α and ϕ_0), particles aggregate towards the free surface, which results in more particles collecting at the leading edge, as evidenced in the bottom row images of Fig. 2.

We have a good understanding of the flow of monodisperse slurries [3, 4] which is well-supported by mathematical analysis both in low particle concentrations [18] and highly-packed suspensions [19]. In order to gain

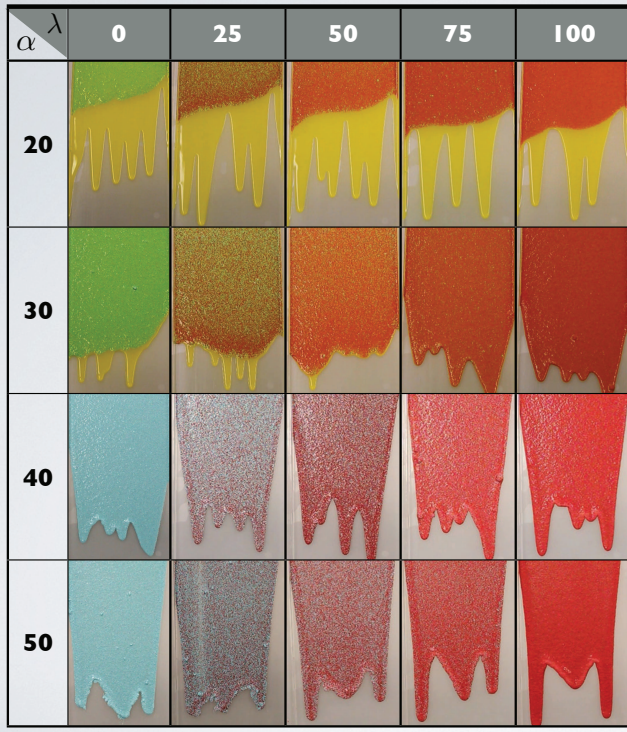


Fig. 2 Phase flow diagram demonstrating the effect of increasing plane angle of inclination (α) and increasing ratio of glass to ceramic beads (λ) on the flow patterns observed experimentally.

some physical insight on the bidisperse slurry dynamics, we examine here the mathematical model for the particle flux, \mathbf{J} , employed in monodisperse suspensions. The model includes both gravitational and shear effects showing excellent agreement with monodisperse experiments [2–4]:

$$\mathbf{J} = d^2 \phi \left[\frac{(\rho_p - \rho_\ell)}{18\mu} f(\phi) \mathbf{g} - \frac{K_c}{4} \nabla(\dot{\gamma}\phi) - \frac{K_v}{4} \frac{\phi \dot{\gamma}}{\mu(\phi)} \nabla \mu \right], \quad (1)$$

where $f(\phi)$ is the hindrance settling function, K_c and K_v are diffusivity constants under shear, $\dot{\gamma}$ is the shear rate, and $\mathbf{g} = g(\sin \alpha, -\cos \alpha)$ is the two-dimensional gravity vector. The first term in Eq.(1) refers to the effects of gravity, while the last two terms correspond to shear-induced migration. Notably, both the settling and shear-induced migration effects scale as d^2 , while only the gravitational term depends on the particle density ρ_p .

To leading order, the physics included in the equilibrium theory for the monodisperse case applies to the bidisperse model as well. Therefore, by including two particle species with approximately equal diameter, d , and two different values of ρ_p in the current experiments, we effectively keep the shear-induced migration

term constant while independently varying the gravitational effects. Thus, the volume ratio between glass and ceramic beads, λ , is expected to affect the overall settling behavior, in addition to α and ϕ_0 . Specifically, increasing the relative amount of heavier ceramic beads (or decreasing λ) should increase the settling effects, as ceramic beads settle faster than glass ones.

In order to illustrate the effects of λ on the overall particle dynamics, a series of bidensity experiments are conducted for $\lambda = 0 - 100\%$, and also for $\alpha = 20^\circ - 50^\circ$, while keeping ϕ_0 constant at 0.4. The results are summarized in Fig. 2: the leftmost and rightmost columns simulate a monodisperse case of ceramic beads (blue) and glass beads (red), respectively. All snapshots are captured at 0.4 m down the inclined plane and cover a distance of 0.25 m. In Fig. 2, moving from left to right, the percentage of glass beads increases (indicated by the increasing value of λ) which results in reduced settling effects. This trend is more evident at intermediate angles; see, for example, the flow regimes corresponding to $\lambda = 25\%$ and $\lambda = 50\%$ at 30° . At lower angles of inclination (refer to rows corresponding to 20° , 30°) the heavier ceramic beads tend to settle fast, while the lighter glass beads move to the front of the flow and, in situations where settling is favored, the clear fluid flows over the particles and advances down the plane. At higher angles of inclination (refer to rows corresponding to 40° , 50°), the particles tend to accumulate at the front of the flow, forming a particle-rich ridge with the heavy particles generally settling first and the lighter particles settling on top of the heavy ones.

The quantitative phase plane in Fig. 3 clearly demonstrates the transition from the settled to ridged regimes: settling is favored for low values of λ and α , and the ridged regime dominates at high λ and α . Each marker point represents a single run; the type of marker reflects the flow regime observed experimentally. The settled, well-mixed, and ridged regimes are represented by circles, triangles, and diamonds, respectively. Based on experimental observations and a confidence interval analysis employing lower and upper limits for the boundary points of each physical regime, we indicate three interval regions on the phase diagram. The dark gray depicts the range of system parameters which result in the ridged regime while the white region shows the range of parameters which favors the settled regime. The lighter gray region represents the intermediate, transient regime. We note that the interval spanning the transient regime is narrower for low values of λ (i.e. increasing volume of P2-type particles); this suggests that decreasing λ induces settling. We find that the onset of settling (this is defined as the first instant at which clear fluid flows over the particles) increases by approximately 50% be-

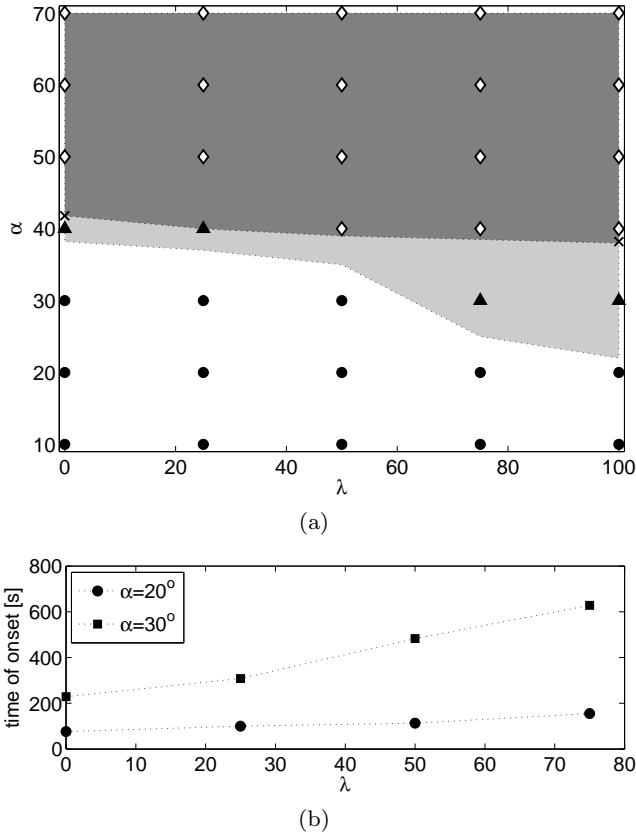


Fig. 3 (a) Phase diagram for fixed *total* particle concentration, $\phi_0 = 0.4$, showing the effect of increasing plane angle of inclination (α) and increasing ratio of glass to ceramic beads (λ). Each marker point represents experimental observations for a single run and the following key is used: circles indicate ‘settled’, triangles indicate ‘well-mixed’ and diamonds indicate ‘ridged’ regimes. The dark gray shaded region shows the range of system parameters within which we expect ridged fronts, the light gray shows the transient regime while the white region represents the range of parameters which favor settling. (b) Plot showing the onset of settling (in seconds) as a function of λ for $\alpha = 20^\circ$ and $\alpha = 30^\circ$.

tween a monodisperse glass suspension ($\lambda = 100\%$) and a predominantly bidisperse suspension ($\lambda = 25\%$) at 20° . We find that, within the ‘settled’ phase space, this trend is more evident at higher inclination angles. This behavior is clearly shown in Fig. 3 (b).

Figure 3 suggests that, while ϕ_0 is kept constant, it is possible to identify a critical angle α_c at which the flow regime behavior changes and is computed here for all ceramic ($\lambda = 0\%$) and all glass ($\lambda = 100\%$) cases. Within the thin film, particles equilibrate in the z -direction (normal to the channel walls) at the leading order (i.e. $J_z = 0$), reducing Eq.(1) to the following [2–4]:

$$\left[1 + k \frac{\phi}{\phi_m - \phi}\right] \sigma \phi' - \frac{2\rho_s \cot \alpha}{9K_c} (1 - \phi) + \sigma' \phi = 0, \quad (2)$$

where $k = 2(K_v - K_c)/K_c$, and $\rho_s = (\rho_p - \rho_l)/\rho_l$, σ is the dimensionless shear stress, and the prime denotes the derivative with respect to z . In addition, ϕ_m is the maximum packing fraction of the mixture which is empirically determined. We solve Eq.(2) together with the fluid flow equation (this is a result of the Stokes equations reduced in the lubrication approximation) as a coupled system of ODEs which yield solutions for the particle concentration, $\phi(z)$ and the slurry velocity, $u(z)$ (refer to [4] for more details on the mathematical model). The resulting ODE solution for $\phi(z)$ shows a bifurcation in the phase space indicating three behaviors associated with the three, aforementioned flow regimes: ϕ monotone decreases in z (settled regime); ϕ monotone increases in z (ridged); ϕ is constant (well-mixed). Therefore, in the well-mixed regime such that $\phi' = 0$ and $\phi = \phi_0$, Eq.(2) can be rearranged to yield the expression for the critical angle α_c , as shown in [3]:

$$\tan \alpha_c = \frac{2\rho_s(1 - \phi_0)}{9K_c\phi_0(1 + \rho_s\phi_0)}. \quad (3)$$

As expected, α_c increases with increasing $\rho_s = (\rho_p - \rho_l)/\rho_l$, as heavier particles settle for a wider range of α . Interestingly, α_c also depends on the value of the diffusivity constant, K_c , which is an empirical measure of how strongly particles experience particle-particle collisions in shear flows [17]. The value of K_c for glass beads is set to be 0.41 from previous experiments [3, 4], while the value of K_c for ceramic is assumed to be higher based on their tendency to form clusters. The evidence of ceramic beads in clusters is highlighted in Fig. 4 for the $\alpha = 50^\circ$ and $\lambda = 0$ case and can also be observed in Fig. 2. According to [20], particles in a cluster act as a single larger particle due to the hydrodynamic lubrication forces, which subsequently forces them to experience higher shear stress and higher collision rate (higher K_c) at a given shear rate. Thus, α_c is computed to be 41.8° for ceramic and 38.2° for glass and is consistent with the experimental results; these are shown in Fig. 3(a) with ‘x’.

We now focus on the separation mechanism between the two particle species by considering a pictorial evolution of the settled regime [Fig. 5 (a)] and the ridged regime [Fig. 5 (b)]. The pictures shown in Fig. 5 cover a distance of 0.65 m from the top of the 0.9 m long track. In both panels the ratio of P1 to P2-type beads is fixed at $\lambda = 25\%$ while the angle of inclination is varied from 30° [panel (a)] to 50° [panel (b)]. Focusing on the ridged regime, the particle front appears evenly mixed with P1 and P2 particles from the onset of the experiment and throughout the run. In the last frame, the leading edge consists of both P1 and P2 particles, which confirms that the dominant shear-induced migra-

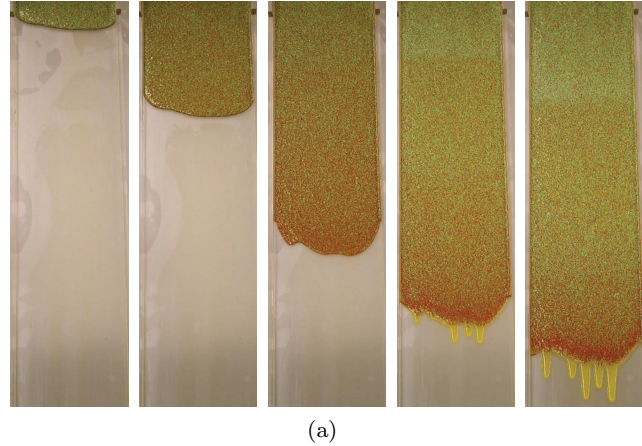


Fig. 4 Enlarged image of the ceramic beads showing clustering at $\alpha = 50^\circ$ and $\lambda = 0$; the circled region shows the more prominent clustering features.

tion effects act equally on P1 and P2 and result in no separation between the species of equal diameter. In the settled regime where gravitational effects dominate, the initially well-mixed front develops over time into three fronts of the clear fluid (yellow fingers), lighter beads (red), and heavier beads (blue), respectively. Within the thin film, heavier P2 beads settle fast before P1 with the clear fluid on top; this stratification due to density differences subsequently evolves into the three aforementioned fronts, resulting in phase separation. We expect the edge delineating the red and blue beads to develop more clearly on a longer track.

4 Discussion

In this paper, we experimentally investigate the behavior of bidisperse slurries flowing down an incline in a thin film. The mixture consists of two negatively buoyant particle species with approximately the same diameter and different densities. This bidensity suspension exhibits three regimes: settled, well-mixed, and ridged, due to the competition of gravitational effects and shear-induced migration. The same regimes have been previously observed in monodisperse slurries in the same geometry for varying channel inclination angle α and the total particle volume fraction, ϕ_0 . However, in the current bidensity study, we observe the transition from the settled to ridged regime even at fixed α and ϕ_0 , by decreasing the volume ratio of light to heavy particles, λ . Specifically, the inclusion of more heavy particles induces settling, which is quantified in two ways. First, as shown on the phase plane [Fig. 3 (a)], decreasing λ results in the suppression of the well-mixed regime



(a)



(b)

Fig. 5 Pictorial evolution of the settled [panel (a)] and ridged [panel (b)] regimes. In both panels, the total particle volume fraction is 40% while the ratio of glass to ceramic beads is fixed at $\lambda = 25\%$. In panels (a) and (b), the plane angle of inclination is fixed at 30° and 50° , respectively. The last frame in panels (a) and (b) is shown after approximately 8 and 4.5 minutes after the gate is released.

(shaded in light gray). Since the well-mixed regime has been theoretically shown to be transient [3,4], the presence of more heavy particles (low λ) minimizes the span of this transient regime, as the settled regime widens. Secondly, for given α and ϕ_0 , the time of onset of settling (when the clear fingers first emerge) increases with increasing λ . This indicates that the addition of heavier particles speeds up the settling behavior, and this effect is more clearly shown for $\alpha = 30^\circ$ in comparison to $\alpha = 20^\circ$ [Fig. 3 (b)], which will be further investigated as future work. In addition, the phase separation between two particle species is observed only in the settled regime [Fig. 5 (a)], in which the dominant gravitational effects stratify the particles by densities. When shear-induced migration effects, which scale with particle size, become important in the ridged regime [Fig. 5 (b)], the particles remain evenly mixed throughout the thin film.

The dynamics of multi-species mixtures is a fundamentally important problem that holds many industrial applications. In particular, the mechanism of phase separation is important in wastewater treatment, crude oil refinement, and mineral processing via a spiral separator. Due to the complex coupling between the particle-fluid dynamics, a rigorous yet tractable model has not yet been developed for these applications. However, as Lee *et al.* [14, 15] showed recently, the monodisperse theory on an incline is valid in spiral geometries, and the resultant particle segregation is determined by the particle dynamics inside the thin film. Therefore, the current experimental results and subsequent work can be directly used to address the particle segregation process in more complex geometries. For instance, the particles of different densities are shown to stratify inside the thin film and develop into three distinct fronts when the sedimentation effects dominate over shear-induced migration. This observation implies that the separation between particle species via a spiral channel is more likely to occur in the settled regime. Thus, future work includes quantitative analysis on the segregation observed in the current experiments and development of the diffusive flux theory for the bidisperse case.

Acknowledgements The authors would like to thank K. Allison, T. Crawford, S. Meguerdijian, and W. Rosenthal for their preliminary work on the bidensity experiments and image processing.

This work was supported by UC Lab Fees Research Grant 09-LR-04-116741-BERA and NSF grants DMS-1312543, DMS-1048840 and DMS-1045536.

References

1. J. J. Zhou, B. Dupuy, A. L. Bertozzi, and A. E. Hosoi. Theory for shock dynamics in particle-laden thin films. *Phys. Rev. Lett.*, 94:117803, 2005.
2. B. P. Cook. Theory for particle settling and shear-induced migration in thin-film liquid flow. *Phys. Rev. E*, 78:045303, 2008.
3. N. Murisic, J. Ho, V. Hu, P. Lattnerman, T. Koch, K. Lin, M. Mata, and A. L. Bertozzi. Particle-laden viscous thin-film flows on an incline: experiments compared with an equilibrium theory. *Physica D: Nonlinear phenomena*, 240, 2011.
4. N. Murisic, B. Pausader, D. Peschka, and A. L. Bertozzi. Dynamics of particle settling and resuspension in viscous liquid films. *J. Fluid Mech.*, 717:203–231, 1 2013.
5. T. Ward, C. Wey, R. Gilden, A. E. Hosoi, and A. L. Bertozzi. Experimental study of gravitation effects in the flow of a particle-laden thin film on an inclined plane. *Phys. Fluids*, 21:083305, 2009.
6. Ancy C., Andreini N., and Epely-Chauvin G. The dam-break problem for concentrated suspensions of neutrally buoyant particles. *J. Fluid Mech.*, 724:95–122, 6 2013.
7. O. Katz and E. Aharonov. Landslides in vibrating sand box: What controls types of slope failure and frequency magnitude relations? *Earth Planet. Sci. Lett.*, 247:280–294, 2006.
8. A. Klar, E. Aharonov, B. Kalderon-Asael, and O. Katz. Analytical and observational relations between landslide volume and surface area *Journal of Geophysical Research: Earth Surface*, 116, 2011.
9. R L Whitmore. The sedimentation of suspensions of spheres. *British Journal of Applied Physics*, 6(7):239, 1955.
10. Ralph H. Weiland and Rodney R. McPherson. Accelerated settling by addition of buoyant particles. *Industrial & Engineering Chemistry Fundamentals*, 18(1):45–49, 1979.
11. RH Weiland, YP Fessas, and BV Ramarao. On instabilities arising during sedimentation of two-component mixtures of solids. *Journal of Fluid Mechanics*, 142:383–9, 1984.
12. R. H. Davis and A. Acrivos. Sedimentation of noncolloidal particles at low reynolds numbers. *Ann. Rev. Fluid Mech.*, 17:91, 1985.
13. Anubhav Tripathi and Andreas Acrivos. Viscous resuspension in a bidensity suspension. *International Journal of Multiphase Flow*, 25(1):1 – 14, 1999.
14. S. Lee, Y. M. Stokes, and A. L. Bertozzi. A model for particle laden flow in a spiral concentrator. In Y. Bai, J. Wang, and F. Daining, editors, *23rd International Congress of Theoretical and Applied Mechanics (ICTAM)*. Procedia IUTAM, 2012.
15. S. Lee, Y. M. Stokes, and A. L. Bertozzi. Particle segregation in spiral channels. preprint.
16. D. Leighton and A. Acrivos. Shear-induced migration of particles in concentrated suspensions. *J. Fluid Mech.*, 181:415, 1987.
17. R. J. Phillip, R.C. Armstrong, R. C. Brown, A.L. Graham, and J. R. Abbott. A constitutive equation for concentrated suspensions that accounts for shear-induced particle migration. *Phys. Fluids A*, 4:30, 1992.
18. A. Mavromoustaki and A. L. Bertozzi. Hyperbolic systems of conservation laws in gravity-driven, particle-laden thin-film flows. submitted to *J. Eng. Math.* (2013).
19. L. Wang and A. L. Bertozzi. Shock solutions for high concentration particle-laden thin films. submitted to *SIAP* (2013).
20. John F. Brady and Georges Bossis. The rheology of concentrated suspensions of spheres in simple shear flow by numerical simulation. *J. Fluid Mech.*, 155:105–129, 5 1985.